Research Article | Vol. 8, No. 6 | 1 Jun 2018 | OPTICAL MATERIALS EXPRESS 1642
Optical Materials EXPRESS

Optical properties of single crystal silver thin films on mica for high performance plasmonic devices

T. UCHINO,[1,*] T. KOIWA,[1] J. Y. OU,[2] AND V. A. FEDOTOV[2]

[1]*Department of Electrical and Electronic Engineering, Tohoku Institute of Technology, Sendai 982-8577, Japan*
[2]*Optoelectronics Research Center, University of Southampton, Highfield, Southampton SO17 1BJ, UK*
t-uchino@tohtech.ac.jp

Abstract: We systematically investigate the optical properties of silver films to clear up the inconsistency in the published values of the dielectric function of silver. The silver films were deposited on mica by using a facing target sputtering system, which yielded a large area single crystal of silver suitable for the fabrication of high-finesse plasmonic devices and metamaterials. We confirmed that wide variations in the optical properties of silver were associated with the overall quality of the silver films including crystal structure, thickness, and surface roughness. The quality factor of the surface plasmon polaritons calculated for the obtained single crystal is 5×10^3, which is about five times higher than that for polycrystalline films.

OCIS codes: (160.3918) Metamaterials; (250.5403) Plasmonics; (310.6860) Thin films, optical properties; (310.6628) Subwavelength structures, nanostructures.

References and links

1. V. G. Veselago and E. E. Narimanov, "The left hand of brightness: past, present and future of negative index materials," Nat. Mater. **5**(10), 759–762 (2006).
2. N. I. Zheludev, "The road ahead for metamaterials," Science **328**(5978), 582–583 (2010).
3. J. B. Pendry, "Negative refraction makes a perfect lens," Phys. Rev. Lett. **85**(18), 3966–3969 (2000).
4. W. Rechberger, A. Hohenau, A. Leitner, J. R. Krenn, B. Lamprecht, and F. R. Aussenegg, "Optical properties of two interacting gold nanoparticles," Opt. Commun. **220**(1–3), 137–141 (2003).
5. N. I. Zheludev, S. Prosvirnin, N. Papasimakis, and V. Fedotov, "Lasing spaser," Nat. Photonics **2**(6), 351–354 (2008).
6. S. A. Maier and H. A. Atwater, "Plasmonics: localization and guiding of electromagnetic energy in metal/dielectric structures," J. Appl. Phys. **98**(1), 011101 (2005).
7. D. A. Bobb, G. Zhu, M. Mayy, A. V. Gavrilenko, P. Mead, V. I. Gavrilenko, and M. A. Noginov, "Engineering of low-loss metal for nanoplasmonic and metamaterials," Appl. Phys. Lett. **95**(15), 151102 (2009).
8. M. G. Blaber, M. D. Arnold, and M. J. Ford, "Optical properties of intermetallic compounds from first principles calculations: a search for the ideal plasmonic material," J. Phys. Condens. Matter **21**(14), 144211 (2009).
9. P. R. West, S. Ishii, G. V. Naik, N. K. Emani, V. M. Shalaev, and A. Boltasseva, "Searching for Better Plasmonic Materials," Laser Photonics Rev. **4**(6), 795–808 (2010).
10. K. Tanaka, E. Plum, J. Y. Ou, T. Uchino, and N. I. Zheludev, "Multifold enhancement of quantum dot luminescence in plasmonic metamaterials," Phys. Rev. Lett. **105**(22), 227403 (2010).
11. M. Kuttge, E. J. R. Vesseur, J. Verhoeven, H. J. Lezec, H. A. Atwater, and A. Polman, "Loss mechanisms of surface plasmon polaritons on gold probed by cathodoluminescence imaging spectroscopy," Appl. Phys. Lett. **93**(11), 113110 (2008).
12. V. A. Fedotov, T. Uchino, and J. Y. Ou, "Low-loss plasmonic metamaterial based on epitaxial gold monocrystal film," Opt. Express **20**(9), 9545–9550 (2012).
13. Y. Wu, C. Zhang, N. M. Estakhri, Y. Zhao, J. Kim, M. Zhang, X. X. Liu, G. K. Pribil, A. Alù, C. K. Shih, and X. Li, "Intrinsic Optical Properties and Enhanced Plasmonic Response of Epitaxial Silver," Adv. Mater. **26**(35), 6106–6110 (2014).
14. C. Y. Wang, H. Y. Chen, L. Sun, W. L. Chen, Y. M. Chang, H. Ahn, X. Li, and S. Gwo, "Giant colloidal silver crystals for low-loss linear and nonlinear plasmonics," Nat. Commun. **6**(1), 7734 (2015).
15. A. A. Baski and H. Fuchs, "Epitaxial growth of silver on mica as studied by AFM and STM," Surf. Sci. **313**(3), 275–288 (1994).
16. T. Mori, T. Mori, Y. Tanaka, Y. Suzaki, and K. Yamaguchi, "Fabrication of single-crystalline plasmonic nanostructures on transparent and flexible amorphous substrates," Sci. Rep. **7**, 42859 (2017).

#320678 https://doi.org/10.1364/OME.8.001642
Journal © 2018 Received 25 Jan 2018; revised 28 Apr 2018; accepted 16 May 2018; published 30 May 2018

Optical Materials EXPRESS

17. S. Buchholz, H. Fuchs, and J. P. Rabe, "Surface structure of thin metallic films on mica as seen by scanning tunneling microscopy, scanning electron microscopy, and low-energy electron diffraction," J. Vac. Sci. Technol. B **9**(2), 857 (1991).
18. M. J. Hall and M. W. Thompson, "Epitaxy and twinning in foils of some noble metals condensed upon lithium fluoride and mica," Br. J. Appl. Phys. **12**(9), 495–498 (1961).
19. N. P. Logeeswaran VJ, M. S. Kobayashi, W. Islam, P. Wu, N. X. Chaturvedi, S. Y. Fang, Wang, and R. S. Williams, "Ultrasmooth silver thin films deposited with a germanium nucleation layer," Nano Lett. **9**(1), 178–182 (2009).
20. Y. Jiang, S. Pillai, and M. A. Green, "Re-evaluation of literature values of silver optical constants," Opt. Express **23**(3), 2133–2144 (2015).
21. H. U. Yang, J. D'Archangel, M. L. Sundheimer, E. Tucker, G. D. Boreman, and M. B. Raschke, "Optical dielectric function of silver," Phys. Rev. B **91**(23), 235137 (2015).
22. Y. Jiang, S. Pillai, and M. A. Green, "Realistic Silver Optical Constants for Plasmonics," Sci. Rep. **6**(1), 30605 (2016).
23. P. B. Johnson and R. W. Christy, "Optical Constants of the Noble Metals," Phys. Rev. B **6**(12), 4370–4379 (1972).
24. P. Nagpal, N. C. Lindquist, S. H. Oh, and D. J. Norris, "Ultrasmooth patterned metals for plasmonics and metamaterials," Science **325**(5940), 594–597 (2009).
25. W. L. Barnes, "Surface plasmon–polariton length scales: a route to sub-wavelength optics," J. Opt. A, Pure Appl. Opt. **8**(4), S87–S93 (2006).
26. S. Kadokura, M. Naoe, S. Nakagawa, and Y. Maeda, "Nano-size magnetic crystallite formation in Co-Cr thin films for perpendicular recording media," IEEE Trans. Magn. **34**(4), 1642–1644 (1998).
27. J. Moon and H. Kim, "Sputtering of aluminum cathodes on OLEDs using linear facing target sputtering with ladder-type magnet arrays," J. Electrochem. Soc. **155**(7), J187–J192 (2008).
28. V. A. Fedotov, M. Rose, S. L. Prosvirnin, N. Papasimakis, and N. I. Zheludev, "Sharp trapped-mode resonances in planar metamaterials with a broken structural symmetry," Phys. Rev. Lett. **99**(14), 147401 (2007).
29. W. P. Davey, "Precision Measurements of the Lattice Constants of Twelve Common Metals," Phys. Rev. **25**(6), 753–761 (1925).
30. M. Higo, K. Fujita, M. Mitsushio, T. Yoshidome, and T. Kakoi, "Epitaxial growth and surface morphology of aluminum films deposited on mica studied by transmission electron microscopy and atomic force microscopy," Thin Solid Films **516**(1), 17–24 (2007).
31. E. Palik, *Handbook of Optical Constants of Solids* (Academic Press 1998).
32. D. J. Nash and J. R. Sambles, "Surface plasmon-polariton study of the optical dielectric function of silver," J. Mod. Opt. **43**(1), 81–91 (1996).
33. J. M. Bennett, J. L. Stanford, and E. J. Ashley, "Optical constants of silver sulfide tarnish films," J. Opt. Soc. Am. **60**(2), 224–232 (1970).

1. Introduction

Plasmonic structures and metamaterials exploiting surface plasmons have attracted great attention over the last decade [1, 2] since they gave rise to some innovative concepts and novel devices such as superlenses, nano-antennas, spasers, and subwavelength waveguides [3–6]. Research on metamaterials operating in the infrared and visible spectral regions is often carried out using metasurfaces rather than their three-dimensional counterparts because of the ease of manufacture. However, the response of the metasurfaces is very sensitive to the presence of dissipative losses in the subwavelength resonators making it difficult to obtain the optimum performance. Several approaches to overcome the losses were investigated, including the search for better plasmonic materials among metallic alloys, heavily doped semiconductors, graphene, and conductive oxides [7–9] in addition to direct compensation of the losses by integrating metamaterials with optical gain media [10]. Although these approaches aim to minimize Joule losses, the actual dissipation rates are often much higher than those expected from Ohm's law. The additional drawback associated with surface roughness and grain boundary scattering due to polycrystalline nature of thin metal films was reported [11]. As a result, employing single crystals of noble metals could become a major step towards the reduction of plasmonic losses. We demonstrated that metamaterials fabricated using epitaxial gold thin films with a surface roughness of less than 0.2 nm showed a strong resonant response in the near-infrared spectral region [12]. Silver is far less expensive than gold and has the lowest intrinsic loss in the visible and near-infrared regions among all metals. Thus, to improve the performance of plasmonic devices and metamaterials, the use of single crystal films of silver is desirable [13–16]. However, silver has low cohesive

Optical Materials EXPRESS

energy as compared with other metals, while silver films on dielectric substrates are easily agglomerated by heating. In fact, it is difficult to obtain continuous silver films with a thickness of 100 nm or less using conventional methods [17–19]. To overcome the difficulty, chemical methods and molecular beam epitaxy techniques have been developed. They enabled the growth of high-quality single-crystal films at temperatures lower than room temperature [13, 14]. Another problem related to the use of silver films stems from an inconsistency in the measured values of the optical dielectric function [20–24]. The dielectric function is important to understand electronic and optical properties of noble metals, especially for transmission and reflection of light. The propagation length of surface plasmon polaritons, plasmon lifetime, and non-radiative loss are directly related to the dielectric function [25]. However, silver has wide variations in the dielectric function associated with sample preparation, measurement techniques, and surface texture. While it is well known that optical properties are affected by surface roughness, grain boundary, and film thickness [11, 12], there have been only a few systematic studies on how film structure affects the optical dielectric function of silver.

In this work, we present a systematic investigation of optical properties of silver thin films deposited by a facing target sputtering system, which yielded large area single crystal thin films. We investigated the effects of film thickness, surface texture, and crystal structure on the optical properties of silver thin films. The deposition conditions were optimized by evaluating the optical characteristics of silver films. We found that the inconsistency in the measured values of the optical dielectric function of silver resulted from the overall quality of the films including crystal structure, thickness, and surface roughness. The obtained single crystal silver thin films allowed us to reduce plasmonic losses and, in contrast to single crystal gold films, extend the useful spectral range to the near ultraviolet wavelengths. The obtained films were also used to fabricate a nanostructured metasurface with a structurally complex pattern, which showed high-Q resonance in the near infrared region. We believe that the silver growth technique, described here, makes it possible to realize inexpensive and low-loss plasmonic systems and devices for various practical applications.

2. Experimental details

Silver thin films were deposited on freshly cleaved mica substrates (Nilaco) with the help of a facing target sputtering system (Biemtron LS-420R), which enabled to avoid plasma damage. The parallel facing target direction was perpendicular to the substrate holder in this system [26, 27]. The substrates were heated during deposition from the back side of the substrate holder. The deposition temperature ranged from room temperature to 500 °C, and the film thickness ranged from 44 to 150 nm. The sputtering was performed at a deposition rate of 2 nm/s and a base pressure of less than 3×10^{-5} Pa. For comparison, we also prepared samples deposited at room temperature on both mica and glass substrates. The mica sheets were cut into pieces of approximately 1×1 cm^2 and freshly cleaved to expose clean and atomically flat surface just before loading into the sputtering system. Mica is a highly transparent dielectric with an exceptionally broad transmission window spanning from UV to mid-IR (0.2 to 10 μm) which makes it an ideal substrate for hosting metamaterial-based optical devices. The glass substrates were cleaned with acetone, isopropanol, and distilled water before the deposition. The thin films were characterized by using various analytical techniques including scanning electron microscopy (SEM), X-ray diffraction (XRD), and high-resolution transmission electron microscopy (HRTEM). The surface morphology of the samples was examined by using atomic force microscope (AFM) operating in a tapping mode under ambient conditions. Spectroscopic ellipsometry measurements using a spectroscopic ellipsometer (J. A. Woollam M-2000) were carried out to extract the optical constants of silver in the wavelength range of 200-1700 nm and at an incidence angle of 60°. The complex dielectric constant $\varepsilon = \varepsilon_1 - i\varepsilon_2$ was obtained from the measured ellipsometric angles Ψ and Δ

Optical Materials EXPRESS

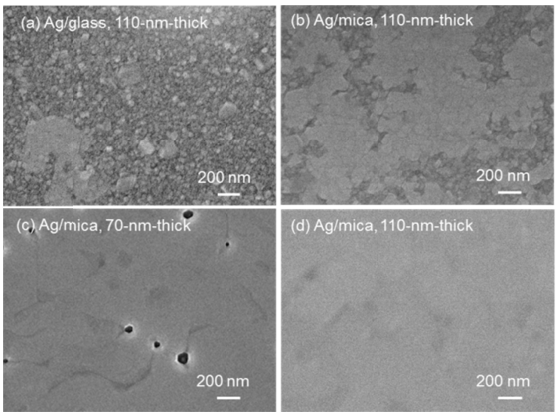

Fig. 1. SEM images of (a) 110-nm-thick silver film deposited on glass at room temperature, (b) 110-nm-thick silver film deposited on mica at room temperature, (c) 70-nm-thick silver film deposited on mica at 500 °C, and (d) 110-nm-thick silver film deposited on mica at 500 °C.

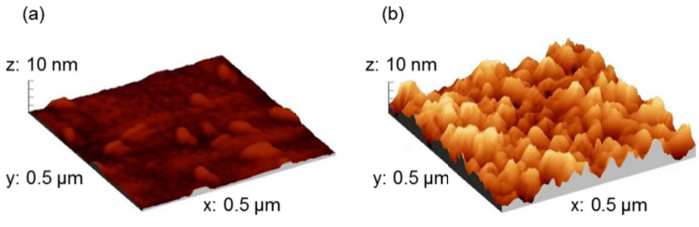

Fig. 2. AFM images of (a) 110-nm-thick silver film deposited on mica at 500 °C. The surface roughness of the film is Rq = 0.6 nm and (b) 110-nm-thick silver films deposited on glass at room temperature. The surface roughness of the film is Rq = 2.5 nm.

as a function of wavelength. The quality factor of surface plasmon polariton (SPP) at the wavelength of 1 μm was evaluated as the ratio of enhanced local field to incident field, which can be expressed as $Qspp = (\varepsilon_1)^2 / \varepsilon_2$ [9].

To demonstrate the full potential of the obtained single crystal silver thin films, we fabricated high-finesse plasmonic metasurfaces using focused ion beam (Helios Nanolab 600). The metasurfaces featured asymmetrically-split-ring pattern, which had been previously used to demonstrate sharp Fano-type resonances in the microwave region [28]. The overall size of the fabricated samples was 23 × 23 μm^2. The metasurfaces were optimized to yield a strong resonance in the telecom-wavelength range, at around 1.4 μm, where the optical response of silver was free from interband transitions [12].

3. Results and discussion

Figures 1(a) and 1(b) show SEM images of 110-nm-thick silver films deposited at room temperature on glass and mica substrates, respectively. Both samples have fine crystal grains, although glass substrates generated even smaller grains compared with the mica substrates. Figures 1(c) and 1(d) show SEM images of the silver films with different thicknesses deposited on mica at 500 °C. The film with the thickness of 70 nm shows holes with the diameter around 100 nm. Given that many holes with diameters ranging from 50 to 200 nm were seen in the film with the thickness of 44 nm (data not shown), we concluded that the density of holes decreased with increasing film thickness. Correspondingly, the silver film with the thickness of 110 nm showed continuous and smooth surface. Thinner films are preferable for the fabrication of high-finesse metamaterials. Although higher deposition temperature is required to achieve epitaxial growth, the continuous silver film with the

Optical Materials EXPRESS

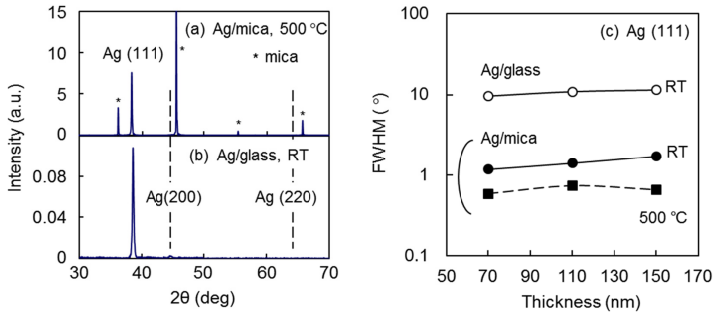

Fig. 3. X-ray diffraction measurement results of (a)110-nm-thick silver film deposited on mica at 500 °C and (b) 110-nm-thick silver film deposited on glass at room temperature. (c) the full width at half maximum (FWHM) of the rocking curve corresponding to silver (111) reflection as a function of film thickness.

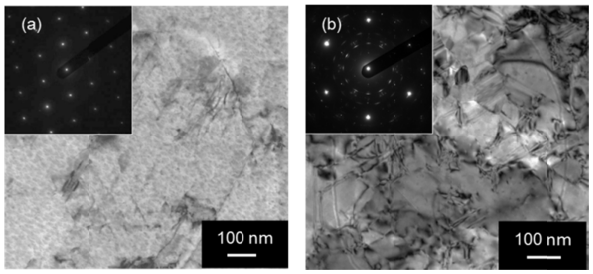

Fig. 4. TEM images and transmission electron diffraction patterns (inset) of silver films deposited at (a) 500 °C and (b) 350 °C.

thickness of 70 nm can be readily obtained with the deposition temperature reduced to 350 °C. Silver thin films deposited on glass substrates had low adhesion to the substrates and could be easily peeled off by heating due to the lower cohesive energy of silver. The adhesion layers of chromium and titanium are often used to deposit silver thin films on glass substrates which, however, deteriorate optical properties of the films. On the contrary, silver films on mica substrates did not come off easily because of van der Waals epitaxy. As the temperature stability of silver films decreases with decreasing film thickness, the aggregation might occur in thinner silver films.

Surface morphology of the deposited silver films was examined over an area of 0.5 × 0.5 μm^2 using AFM. Figure 2 shows typical AFM image of a 110-nm-thick silver/mica film deposited at 500 °C. For comparison, the surface morphology of the silver/glass film deposited at room temperature is also presented. The silver/mica film deposited at 500 °C has a smooth surface with the average root mean square of roughness Rq = 0.6 nm. In contrast, the silver films deposited at room temperature have even rougher surfaces. The surface roughness of silver/glass samples and silver/mica samples are 2.5 nm and 1.7 nm, respectively. The surface roughness increases with increasing thickness of silver films for both mica and glass substrates. Baski *et al.* found that higher deposition rate of 4 nm/s and high substrate temperature around 350 °C made it possible to epitaxially grow silver films with the atomically flat surface over micron regions [15], which is consistent with our results.

Figures 3(a) and 3(b) show the X-ray diffraction results for silver thin films. The film deposited on mica substrate exhibits strong diffraction peaks corresponding to silver (111) crystal plane in addition to peaks from the mica substrate. The lattice constant of the silver film estimated from the peak position was 4.06 Å, which is in good agreement with previous data [29]. By contrast, the silver film deposited on a glass substrate exhibits weak diffraction

Optical Materials EXPRESS

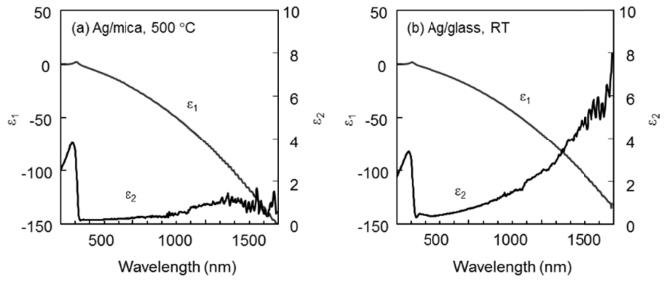

Fig. 5. Spectroscopic ellipsometry measurement results of silver films deposited on (a) mica at 500 °C and (b) glass deposited at room temperature. The real (ε1) and imaginary (ε2) parts of the dielectric function were retrieved from measured Ψ and Δ.

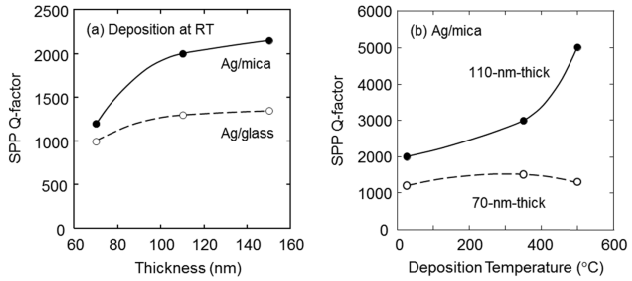

Fig. 6. The quality factors of surface plasmon polaritons (SPP) estimated using the measured optical constants. SPP quality factors as a function of (a) film thickness and (b) deposition temperature.

peaks associated with silver (111) and (200) crystal planes, which indicates that the film was polycrystalline. Figure 3(c) shows the full width at half maximum (FWHM) of the rocking curve corresponding to silver (111) reflection as a function of the film thickness. FWHM of the silver film on a glass substrate is about ten times larger than that of the silver film on a mica substrate due to small crystallite size. FWHM of the silver film deposited on a mica substrate at 500 °C is less than one degree, indicating that high-temperature deposition improved crystalline quality.

The crystal structure of silver films was analyzed by HRTEM. The silver thin films were peeled off from mica substrates using adhesive tape, and the detached films on the TEM grids were thinned to about 50 nm using ion beam milling and wet etching for high-resolution imaging. Figure 4(a) shows typical TEM image of the silver film deposited at 500 °C and a transmission electron diffraction pattern taken from an area with the diameter of 1 μm. Six-fold symmetry spots are seen in the diffraction pattern, which indicates that the silver film is (111) oriented fcc single crystal. Figure 4(b) shows the results for the silver film deposited at 350 °C. Some grains are seen in the plan view, and six-fold symmetry spots along with additional weak spots are observed in the diffraction pattern. These results indicate that the silver films deposited at 350 °C consist of large crystals with (111) plane and randomly oriented column grains. Higo *et al.* reported similar results for aluminum films deposited on mica substrates by thermal evaporation and concluded that the aluminum films deposited in the temperature range from 250 to 450 °C exhibited polycrystalline structure, while epitaxial films could be obtained at a temperature of 500 °C [30].

Figure 5 shows the results of spectroscopic ellipsometry measurements for single crystal and polycrystalline silver films. The real (ε_1) and imaginary (ε_2) parts of the dielectric constant are plotted in the wavelength range from 200 to 1700 nm. Both silver films show strong interband transitions in the ε_2 spectra at the wavelength of 300 nm. The values of ε_2 corresponding to single crystal silver film, which are relevant to the level of plasmonic losses

Optical Materials EXPRESS

in the metal, are smaller than those in the case of polycrystalline silver film. This result is consistent with the fact that the electron scattering due to surface roughness and grain boundaries in polycrystalline metal films causes losses [11] and, hence single crystal silver film should have a lower loss in the visible and near-infrared region. The obtained values of ε_2 are comparable to those recently reported for silver films grown by molecular beam epitaxy (MBE) [13] and smaller than previously published values including widely used data by Johnson and Christy [23, 31, 32].

The quality factors of SPP for all samples were estimated using the measured dielectric permittivity. Figure 6(a) shows the quality factors of SPP at the wavelength of 1 μm as a function of the thickness of silver films deposited at room temperature. The quality factors corresponding to silver films on mica are seen to increase with increasing film thickness, and their values are about two times larger than those in the case of silver films on the glass when the film thickness exceeds 100 nm. On the other hand, silver films on glass are characterized by only a small increase in the quality factors for thicker samples. These results are consistent with the previous results [11] and suggest that the penetration of SPPs into single crystal films is deeper than into polycrystalline ones. Correspondingly, the presence of grain boundaries and surface roughness lead to the reduction of the quality factors of SPP. Figure 6(b) shows the quality factors of SPP for the silver films on mica as a function of deposition temperature. The quality factor corresponding to the single crystal silver film with 110-nm-thick is around 5×10^3, which is about five times higher than the value of the commonly used silver film on glass. The drastic increase in the quality factors is seen around 350 °C in the case of 110-nm-thick silver films, which is attributed to the transition from polycrystalline to the single crystal structure. As for 70-nm-thick silver films, the deposition at temperatures above 350 °C causes the formation of voids on the film surface, and consequently, the quality factor was reduced.

As an additional quality test for the obtained single crystal silver films, we investigated plasmonic metasurfaces exhibiting sharp Fano resonances. Figure 7(a) shows an SEM image of a high-finesse plasmonic metasurface fabricated in a 110-nm-thick single crystal silver film deposited at 500 °C. The metasurface is formed by an array of 40 nm wide slits shaped in the form of asymmetrically-split rings (ASR). The radius of the rings is 120 nm and the period of the array is 320 nm. The long and short arcs have the length of 377 and 272 nm and are separated by narrow gaps of about 53 nm. Figure 7(b) shows the reflection spectra of the fabricated metasurface. The spectra feature a Fano resonance at around 1.4 μm, which are similar results of the previously demonstrated ASR metasurface using epitaxial gold films on LiF substrates [12]. Remarkably, the resonances from both 110-nm-thick silver films and 80-nm-thick gold films have the same Q-factors even though the volume of ASR metamolecules in the silver metasurface is larger by about 40%. This result indicates that intrinsic loss in the obtained silver films was substantially lower than that in the epitaxial gold films, suggesting high quality. The endurance of the silver films is great concerns in practical use. The dot-and-dash line in Fig. 7(b) shows the reflection spectrum of the silver ASR metasurface after leaving the sample in air for nine months. The aged silver ASR metasurface exhibits an almost identical reflection spectrum with only a slight red-shift. Exposing the sample to high vacuum did not affect the spectrum, which suggested that the red shift could not have resulted from the accumulation of moisture. The other possible explanation was that over time a certain fraction of silver in the film had been transformed into silver sulfide. To test the conjecture, we performed an energy dispersive X-ray spectroscopy (EDX) analysis of the sample. It revealed the presence of 0.5% of sulfur on the background of 67% of silver (with the remaining 32.5% taken mostly by aluminum and oxygen, which came from the mica substrate). Given that the thickness of the silver film was 110 nm, the detected amount of sulfur would be equivalent to a 0.8-nm-thick surface layer of silver sulfide, which is a monolayer of the compound. Such a thin surface layer

Optical Materials EXPRESS

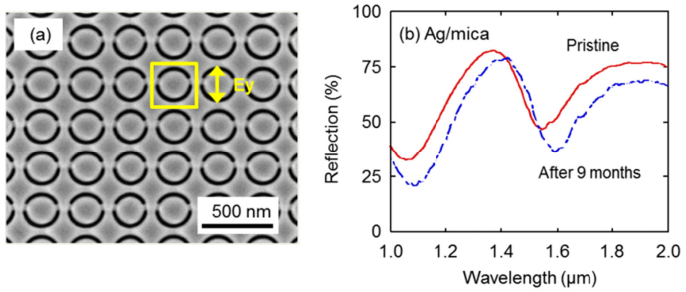

Fig. 7. High-finesse plasmonic metamaterial fabricated on a 110-nm-thick single crystal silver film grown at 500 °C. (a) SEM image of the metamaterial. Yellow box shows elementary unit cell of the periodic pattern. (b) Reflection spectra of the pristine (solid line) and aged (dot-and-dash line) metamaterial.

would naturally cause a small red shift in the spectrum due to the high refractive index of silver sulfide [33]. At the same time, it was too thin to increase absorption in the metamaterials, which might explain the seeming stability of single crystal silver films regarding their optical performance. The formation of only a monolayer of silver sulfide was also consistent with the absence of grains. Indeed, in the case of a polycrystalline film, silver sulfide would have penetrated into the silver film along with the grain boundaries which increases the relative composition of sulfur in EDX analysis. Although further investigation is required, single crystal films appear to be stable due to the absence of grain boundaries.

4. Conclusion

A systematic investigation of optical properties of silver thin films deposited by a facing target sputtering system has been carried out. We found that the extracted optical dielectric function of silver depends on the overall quality of the films including such characteristics as crystal structure, thickness, and surface roughness which are held responsible for the inconsistency with previously reported data sets. The deposition conditions were optimized by evaluating the optical characteristics, and it was demonstrated that single crystal silver thin films enabled a substantial reduction of plasmonic losses. In particular, the SPP quality factor of a single crystal film with 110-nm-thick reached 5×10^3, which was about five times higher than that of commonly used silver films on glass. We believe that the described silver film deposition technique holds promise not only for the fabrication of large-scale plasmonics and metamaterial devices but also for crystal growth of two-dimensional materials.

Funding

JSPS KAKENHI (JP25390100).

Acknowledgments

This work was carried out under the Cooperative Research Project Program of RIEC, Tohoku University. The authors acknowledge Dr. Ikeda, NIMS for assistance with sputtering, and Dr. Konishi, University of Tokyo for help with ellipsometry measurements in Nanotechnology Platform Project sponsored by MEXT, Japan.